Inelastic state-to-state scattering of OH ($^2\Pi_{3/2}, J=3/2, f$) by HCl

R. Cireasa[a)]
Department of Applied Physics, Institute of Molecules and Materials, Radboud University Nijmegen, Toernooiveld 1, 6525 ED Nijmegen, The Netherlands

M. C. van Beek
Philips Research Laboratories, Prof. Holstlaan 4, 5656 AA Eindhoven, The Netherlands

A. Moise and J. J. ter Meulen
Department of Applied Physics, Institute of Molecules and Materials, Radboud University Nijmegen, Toernooiveld 1, 6525 ED Nijmegen, The Netherlands

(Received 2 November 2004; accepted 17 November 2004; published online 10 February 2005)

Parity resolved state-to-state cross sections for inelastic scattering of OH ($X^2\Pi$) by HCl were measured in a crossed molecular beam experiment at the collision energy of 920 cm^{-1}. The OH ($X^2\Pi$) radicals were prepared in a single quantum state, $\Omega=3/2$, $J=3/2$, $M_J=3/2$, f, by means of electrostatic state selection in a hexapole field. The rotational distribution of the scattered OH radicals by HCl was probed by saturated LIF spectroscopy of the 0-0 band of the $A^2\Sigma^+-X^2\Pi$ transition. Relative state-to-state cross sections were measured for rotational excitations up to $J=9/2$ within the $\Omega=3/2$ spin–orbit manifold and up to $J=7/2$ within the $\Omega=1/2$ spin–orbit manifold. A propensity for spin–orbit conserving transitions was found, but no propensity for excitation into a particular Λ-doublet component of the same rotational state was evident. The data are presented and discussed in comparison with results previously obtained for collisions of OH with CO ($E_{coll}=450$ cm^{-1}) and N_2 ($E_{coll}=410$ cm^{-1}) and with new data we have measured for the OH+CO system at a comparable collision energy ($E_{coll}=985$ cm^{-1}). This comparison suggests that the potential energy surface (PES) governing the interaction between OH and HCl is more anisotropic than the PES's governing the intermolecular interaction of OH with CO and N_2.
 [DOI: 10.1063/1.1846692]

I. INTRODUCTION

Due to its abundance and reactivity, the OH radical is responsible for many chemical processes relevant for atmospheric and combustion chemistry.[1,2] Reactions of OH with H_2 and CO are important steps in the reaction chain of hydrocarbon/air flames. Concerning the chemistry of the Earth's atmosphere, reactive OH acts as an efficient scavenger for trace pollutants present in the troposphere and stratosphere. Reactions of OH with hydrogen halides, which are the major sinks for the halogens from the atmosphere that can participate in catalytic ozone destruction in the stratosphere, are known to be efficient reconverters of the halogens to the active forms. In particular, the OH+HCl reaction is the primary process that releases active chlorine in the atmosphere. Therefore, the rate of chlorine release from HCl controls the steady state Cl concentration in the stratosphere. In addition, the formation of HCl serves as the predominant chain termination step for the ClO_x catalyzed destruction of ozone.

The important role played by the OH+HCl reaction in the atmospheric chemistry has given rise to a wealth of experimental and theoretical studies of the reaction dynamics of this system. Quantitative information on the reactivity of the OH+HCl system is provided by an extensive set of kinetic experiments in which temperature dependent rate constants were measured in a wide temperature range.[3–10] The several theoretical studies reported to date, approached the OH+HCl system at different levels of theory in order to develop the Potential Energy Surface (PES) governing the interaction and to calculate rate constants and reaction cross sections.[11–15] Clary *et al.*[11] performed quantum scattering calculations using the Rotating Bond Approximation (RBA) and a semiempirical potential energy surface with a classical energy barrier of 0.25 kcal/mol. Steckler *et al.*[12] applied variational transition-state theory using scaled *ab initio* electronic structure calculations to determine the minimum energy path (MEP). Using the Coupled Cluster with Single, Double, and Triple excitation method (CCSD(T)/PVQZ) method they obtained a vibrational adiabatic ground-state reaction barrier (V_a^G) of 2.65 kcal/mol. Yu and Nyman[13] carried out dynamical calculations using the RBA approach on a new PES obtained by interpolation of *ab initio* energy values computed using the Unrestricted Møller–Plesset method (UMP2) and scaling correction. The ground-state surface $^2A'$ calculated by Yu and Nyman exhibits a deep van der Waals well of −5.46 kcal/mol relative to the OH+HCl reactants possibly due to the strong dipole–dipole interactions and an early barrier (V_a^G) of 2.32 kcal/mol. The most recent theoret-

[a)]Present address: Physical and Theoretical Chemistry Laboratory, University of Oxford, South Parks Road, Oxford OX1 3QZ, United Kingdom. Permanent address: Laser Department, National Institute for Laser, Plasma, and Radiation Physics, P.O. Box MG-36, Bucharest, Romania. Electronic mail: H.terMeulen@science.ru.nl

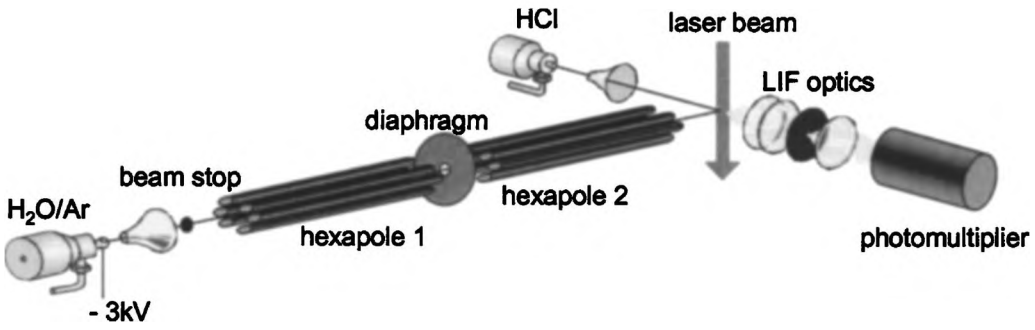

FIG. 1. The schematic representation of the experimental setup used to measure state-to-state inelastic collisions.

ical calculations[14,15] used the Large Angle Rotating Bond (LAGROBO) functional formulation of the interaction between OH and HCl in order to produce the PES. Parameters of the PES were adjusted in order to minimize the difference between the values of the rate constants obtained using quasiclassical trajectory (QCT) calculations and experimental values. The best agreement with experiments was obtained for a PES with a classical barrier of 2.43 kcal/mol and a van der Waals well of −5.45 kcal/mol.

The connection between reactive and inelastic scattering for systems with highly attractive PES like OH+HCl is quite strong because the alternate complex formation/decomposition route to the inelastic process can also be regarded in a broader sense as a reactive event. A systematic study of both types of collisions is particularly fruitful in revealing the multifaceted nature of the collision dynamics and in testing the PES's developed to describe it. In spite of the great number of studies concerning the reactivity of this system, no experiments were reported so far for the state-to-state scattering of OH by HCl and the development of a PES suitable for calculations on the non-reactive channel was just lately approached.[16] Very recently, close coupling scattering calculations and quasiclassical trajectory calculations were performed by Klos *et al.* using only the V_{sum} (see Sec. V) of the PES, the results of which were compared with our experimental cross sections by ignoring their fine-structure.[17] Currently the accuracy of different features of this PES is refined in order to allow for state-resolved quantum scattering calculations.

In this paper we present a study of the inelasticity of the scattering of OH ($X^2\Pi$) by HCl ($X^1\Sigma^+$) in a crossed molecular beam set-up at collision energies around 920 cm^{-1}. Prior to collisions, the OH radicals are selected in a single quantum state, i.e., $\Omega=3/2$, $J=3/2$, $M_J=3/2$, *f*. In the absence of other experimental and theoretical information concerning inelastic collisions of OH with HCl, we compare our data with results previously obtained by using a similar experimental set-up for the collisions of OH with CO ($E_{\text{coll}}=450$ cm^{-1}) and N_2 ($E_{\text{coll}}=410$ cm^{-1}). In order to make the comparison more relevant, we performed new measurements on the OH+CO system at a collision energy $E_{\text{coll}}=985$ cm^{-1}, comparable to that used in the OH+HCl experiments. Relative state-to-state cross sections were measured for rotational excitations up to $J=9/2$ within the $\Omega=3/2$ spin–orbit ladder and up to $J=7/2$ within the $\Omega=1/2$ spin–orbit ladder. Information on the anisotropy of the interaction potential is inferred from the observed propensities for scattering into a particular Λ-doublet state, *e* or *f*. Additional information on the PES anisotropy will be reported in a subsequent paper investigating the effect of the relative orientation of the collision partners on the collision outcome. Favorable orientations of the OH molecule with respect to HCl may enhance possible competing effects implying reactive collisions when the collision energy exceeds the reaction barrier.

II. EXPERIMENTAL SET-UP

The experiments were carried out in a crossed molecular beam machine which is described extensively in previous papers[18–21] and schematically depicted in Fig. 1. Therefore, we will only give a brief description highlighting the features relevant to the experiments reported here. Both molecular beams were obtained by using pulsed current loop valves (Jordan Inc.) with a pulse width of 40–50 μs. The OH beam was produced by means of a pulsed discharge in a mixture of about 4% H_2O vapor and Ar (backing pressure of 600 Torr) established at the exit of a 0.2 mm diameter nozzle. The rotational cooling ($T_{\text{rot}}\approx 35$ K) created in the supersonic expansion was insufficient for accurate state-to-state scattering measurements. In order to improve the initial state preparation we used the electrostatic state selection method to prepare the OH radicals in a single quantum state. An extensive description of this method is given in Refs. 21–24. For this purpose, a system consisting of a double hexapole combined with a beam stop and a diaphragm was used to focus only the OH radicals in the $\Omega=3/2$, $J=3/2$, $M_J=3/2$, *f* state, into the collision region located 36 cm away from the nozzle exit. A positive voltage of 23 kV was applied to every other rod of the hexapoles, while the other rods were grounded. The initial state distribution was determined from saturated Laser-Induced Fluorescence (LIF) measurements of the appropriate rotational transitions of the $A^2\Sigma^+(v'=0)-X^2\Pi(v''=0)$ system. It was found that 93.3% of molecules were in the $\Omega=3/2$, $J=3/2$, *f* state, 4% in the $\Omega=3/2$, $J=5/2$, *f* state with the remaining molecules being distributed over different rotational states (less than 0.5% per quantum state). The ratio of M_J state populations, $|M_{J=3/2}|/|M_{J=1/2}|$, in the $J=3/2$ state was determined to be 15.8. The velocity of the OH beam was determined to be 885 m/s with a spread (FWHM) of 160 m/s from LIF measurements of the time-dependent OH distribution at different distances from the nozzle. The HCl

beam was obtained by expanding pure HCl through a 0.5 mm diameter nozzle. A stagnation pressure of 530±30 Torr was chosen to ensure the single collision regime. A rotational temperature of 20±5 K was inferred from REMPI (1+1′) measurements of the $V^1\Sigma^+ - X^1\Sigma^+$ transition at 118 nm. At a distance of 85 mm from the nozzle exit, the HCl beam was crossed at right angle by the OH beam. For this geometry, the collision energy was estimated to be 920 cm^{-1} with a spread at FWHM of 250 cm^{-1}.

The collision outcome was probed by measuring the OH population distribution over the different rotational states of the ground electronic state using the saturated LIF method. The radiation of 308 nm used for the excitation of the (0-0) band of the $A^2\Sigma^+ - X^2\Pi$ transition was obtained by frequency doubling the output of a dye laser (Continuum TDL-60) operating with Sulforhodamine 640 and pumped by a Nd:YAG laser (Continuum 681 C). The laser pulse energy was attenuated to 0.5–0.8 mJ/pulse to avoid power broadening effects. Hence, the spectral resolution was limited by the laser bandwidth at 0.45 cm^{-1}. Light baffles were used to define a homogeneous detection region, by cutting off the low-energy laser wings, which would not have allowed saturating the transition. The population of the upper Λ-doublet states, states of f symmetry, was probed by Q_1 or P_2 transitions whereas the population of the lower Λ-doublet states, states of e symmetry, was probed by P_1 or Q_2 transitions. Because the $Q_2(2)$ and $Q_2(3)$ lines cannot be resolved within the laser bandwidth, the populations of both states, $\Omega=1/2$, $J=3/2$, e and $\Omega=1/2$, $J=5/2$, e, were measured simultaneously. The OH fluorescence signal was collected by a system of lenses, spatially filtered by a diaphragm and imaged onto a photomultiplier tube (EMI 9235QB). A black cone and a Schott UG-11 filter were inserted in front of the imaging optics with the purpose of suppressing stray light and visible radiation emitted in the discharge. The signal was first amplified 5 times and then integrated with a gated boxcar averager. All measurements were performed at 10 Hz with the laser wavelength parked at the transition peaks. The discrimination between the initial state population and the collision induced population was made by modifying the delay of the HCl beam every 128 laser shots from 0 to 10 ms. For each measurement, an averaging over 1000 laser shots was performed in order to obtain the collision signal. Generally, 5–15 measurements were performed for each rotational state. The measurement errors were in the order of 5%–10% for most of the rotational states, except for the states with weaker excitation cross sections for which they ranged up to roughly 40%.

III. DATA ANALYSIS

As shown previously,[25] the relative state-to-state collision cross section, $\sigma_{i\to f}$, for scattering out of the initial state i into a final state f can be calculated using the following formula:

$$\sigma_{i\to f} \propto \frac{\delta S_{ff'}}{n_i \cdot L_{ff'} \cdot P_{ff'} \cdot F_f}, \tag{1}$$

in which $\delta S_{ff'}$ represents the scattering signal, obtained by subtraction of the fluorescence signal corresponding to the initial population from the fluorescence signal corresponding to the final population of the state f, n_i represents the population density of the initial state before collisions, $L_{ff'}$ represents the rotational line strength of the transition used to probe the f state, $P_{ff'}$ is the laser power at the excitation frequency and F is the flux-to-density transformation factor. Because the scattering signals were measured under saturation conditions, the $L_{ff'}$ and $P_{ff'}$ factors are, in fact, independent of the rotational states probed and can be ignored. The detection geometry employed in this experiment allows us to ignore the flux-to-density transformation as the dimension of the laser spot exceeds the interaction region ensuring the detection of all the scattered molecules. Another argument in favor of neglecting the flux-to-density transformation is the relatively small difference, less than 40%, in the kinetic energy release for the molecules scattered over different rotational states. In the saturation limit and in the absence of a well defined laser polarization, the rotational state populations can be directly determined from the fluorescence signals by dividing them by the excitation rate factors,[26–28]

$$f = \frac{2J'+1}{(2J'+1)+(2J''+1)}, \tag{2}$$

where J'' and J' represents the initial and the final state rotational quantum number of the transition, respectively. When the ρ-doublet splitting was not resolved, the saturation of both main and satellite lines was taken into account for the calculation of the excitation rate factor.

Therefore, according to these considerations, relative cross sections can be derived directly from the ratios between the collision induced populations of the f state and the population of the initial state, i, before collisions. In the determination of the relative state-to-state cross sections, we have assumed that the scattering signal is due only to the scattering of molecules out of the $\Omega=3/2$, $J=3/2$, f state. Contributions to the scattering out of $\Omega=3/2$, $J=5/2$, f state or other weakly populated states were ignored as their contribution was estimated to be insignificant. In turn, the outscattering from $\Omega=3/2$, $J=5/2$, f was accounted for in the calculation of the relative cross section for the excitation into this rotational state. Hereto, it was assumed that the percentage of outscattered molecules from the $J=5/2$, f state was the same as for the scattering from the $J=3/2$, f state.

The final values for the relative state-to-state cross sections were obtained from averages over a different number of measurements. Since the error bars of the individual measurements for the same rotational state were different, we have used a weighted statistical analysis.

IV. RESULTS AND DISCUSSIONS

The values of the relative integral state-to-state cross sections measured in this experiment are listed in Table I and shown graphically in Fig. 2. They are presented together

TABLE I. Relative state-to-state cross sections for inelastic collisions of OH with HCl presented in comparison with cross sections obtained for the scattering of OH by CO and N_2 (Ref. 20). The cross sections for OH+CO and OH+N_2 are scaled to each other as described in Ref. 20, but no scaling procedure was performed for OH+HCl cross sections. The errors represent one standard deviation and for OH+HCl were obtained by a weighted statistical analysis.

Final state			OH+HCl	OH+CO	OH+N_2
Ω	J'	$\in$	E_{coll}=920 cm^{-1}	E_{coll}=450 cm^{-1}	E_{coll}=410 cm^{-1}
3/2	3/2	*e*	55.36±1.43	50±5	40±4
	5/2	*e*	6.28±0.21	5.2±0.6	4.9±0.5
	5/2	*f*	6.48±0.28	4.0±0.4	1.96±0.20
	7/2	*e*	1.76±0.15	1.10±0.11	0.74±0.08
	7/2	*f*	1.75±0.16	1.22±0.13	0.71±0.08
	9/2	*e*	0.49±0.10	0.77±0.03	0.27±0.06
	9/2	*f*	0.82±0.30	0.12±0.04	0.07±0.01
1/2	1/2	*e*	1.49±0.08	1.46±0.15	1.4±0.3
	1/2	*f*	1.47±0.20	1.23±0.13	1.00±0.10
	3/2 and 5/2	*e*[a]	1.78±0.12	1.02±0.11	0.67±0.07
	3/2	*f*	0.83±0.08	0.71±0.09	0.56±0.08
	5/2	*f*	1.3±0.24	0.45±0.05	0.08±0.04
	7/2	*e*	0.87±0.10	···	···

[a]The measured cross section contains contributions from both 3/2 *e* and 5/2 *e* states as the absorption lines used to probe them could not be resolved within the laser bandwidth.

with the cross sections measured for inelastic scattering of OH by N_2 and CO.[20] As can be noted from the table, rotational excitation of the OH radical into states up to J=9/2 of the same spin–orbit ladder, Ω=3/2, and J=7/2 of the upper spin–orbit ladder, Ω=1/2, could be detected within the sensitivity of this experiment. The maximum internal excitation requires only approximately 40% of the available collision energy of 920 cm^{-1}. The rotational energy transfer (RET) seems low in comparison to that measured for OH+N_2 and OH+CO collisions, for which the maximum conversion corresponds to 83% and 75% of the available collision energy of 410 cm^{-1} and 450 cm^{-1}, respectively. Similar high conversion rates of the collision energy into internal excitations were obtained for OH collisions with He, Ar, and CO_2 at low collisions energies,[18–20] and for NO collisions with He and Ar.[29] Besides a genuine "inefficient" RET, several other factors may be responsible for this low conversion rate. Generally, the S/N ratio for the measurements of the excitation into higher J states, for which the cross sections are smaller, is decreasing making the detection difficult. Moreover, for the OH+HCl system, we also have to take into account that for collision energies above the reaction barrier, reactive processes may play a role in the dynamics. The reaction barrier was predicted to lie between 850 and 915 cm^{-1}, but some comparisons of the TS rate constants to the experimental values suggested that the real value might be as low as 350 cm^{-1}.[11–15] Therefore, the collision energy of 920 cm^{-1} used in this experiment is likely to exceed the reaction barrier. If reactions do take place, the collision-induced populations of higher rotational states may drop below the detection limit.

As can be seen from Fig. 2, the behavior of the relative cross sections with the amount of rotational excitation, ΔE_{rot}, appears to obey an energy gap law: its magnitude is decreasing as ΔE_{rot} increases. This is qualitatively similar to the trend obtained for OH+CO and OH+N_2 collisions, except for the values measured for excitation into higher rotational

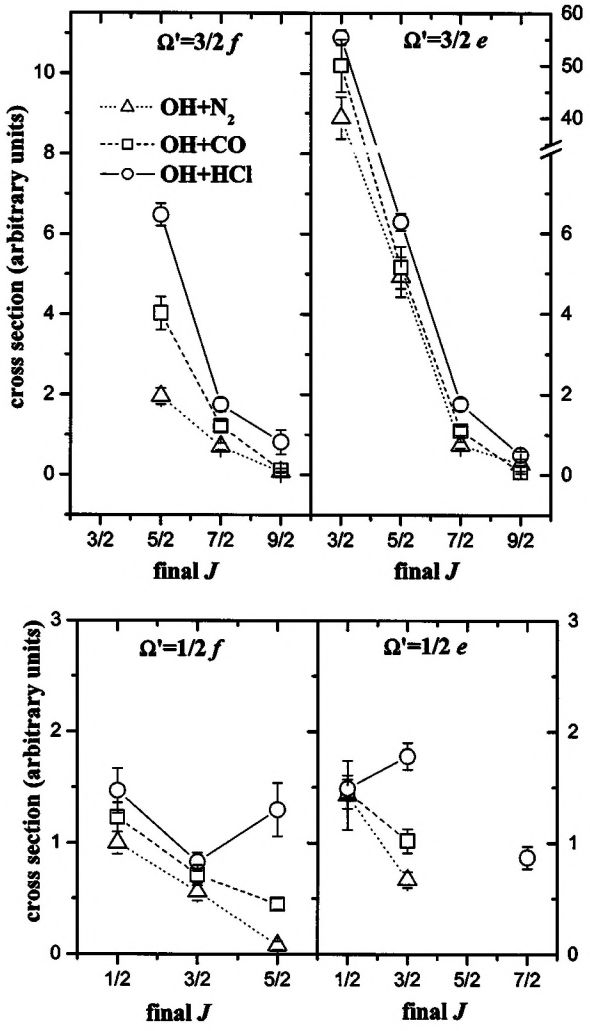

FIG. 2. Rotational dependence of the relative state-to-state cross sections for inelastic collisions of OH with HCl, CO, and N_2 at collision energies of 920 cm^{-1}, 450 cm^{-1}, and 410 cm^{-1}, respectively. The final spin–orbit state and the Λ-doublet symmetry are indicated at the top each panel.

TABLE II. Polarity of HCl vs CO and N_2.

Polar character	HCl	CO	N_2
Dipole moment (D)	1.09	0.11	0
Quadrupole moment (10^{-26} esu cm^2)	3.5	−2.7	−1.4
Polarizability (10^{-24} cm^3)	2.63	1.95	1.74

states of the $\Omega=1/2$ spin–orbit ladder. The Λ-doublet cross section for the de-excitation from the $\Omega=3/2$, $J=3/2$, f state into the $\Omega=3/2$, $J=3/2$, e state is larger than expected from an energy gap law dependence even for a small Λ-doublet splitting. This effect was also observed for OH molecules colliding with CO and N_2 as well as other atomic or di- and triatomic partners, except for He.[18–21] A propensity for spin–orbit conserving transitions is apparent when similar amounts of rotational excitation are considered. Generally, the same propensity was found for collisions of OH with Ar, He, N_2, CO, and CO_2.[18–21] Notably, for the OH+HCl system, no evident propensity for excitation into a particular Λ-doublet component of the same rotational state was measured except perhaps for the $\Omega=3/2$, $J=9/2$ state. The same behavior was found for collisions of OH with CO, but not for collisions with N_2 or atomic partners, Ar and He,[18–21] for which the propensity for scattering into rotational states of e symmetry is very marked. If the de-excitation into the $\Omega=3/2$, $J=3/2$, e state is not taken into account, the ratios between the sum of the cross sections for scattering into states of e symmetry and the sum of the cross sections for scattering into states of f symmetry within the same spin–orbit ladder, $\Omega=3/2$, are 0.94, 1.2, 2.2, 9.4, and 6.3 for collisions with HCl, CO, N_2, Ar, and He, respectively. The same trend of the e/f cross section ratio was found for scattering into the $\Omega=1/2$ spin–orbit component, though the propensity is weaker: 0.91, 1.0, 1.3, 2.3, and 2.6. It seems that the e/f cross section ratios are in line with the polarity of the collision partner. The most spherical symmetric collision partner has the highest propensity for scattering into states of e symmetry, while for the most polar molecule there is no propensity.

In the absence of theoretical calculations, absolute integral state-to-state cross sections cannot be extracted from the measurements. Concerning the absolute magnitudes of the state-to-state cross sections for the OH+HCl collisions, one should expect higher values than for the other two systems, given the stronger polar character and the higher polarizability of HCl as compared with CO and N_2 (see Table II) and the consequently stronger intermolecular interactions. From Table I, it would appear that the cross sections for OH+HCl are larger for the same final state J than those for the other two systems listed. However, given that the tabulated values represent relative cross sections and that both the collision energies and the beam densities were quite different in the three sets of experiments, a genuine quantitative comparison is not possible. For a quantitative comparison, new measurements were performed for the OH+CO system under the same experimental conditions and thus at comparable collision energies. The relative state-to-state cross sections for the OH+HCl system are presented together with the new data obtained for collisions of OH with CO in Table III and Fig. 3. In order to make the comparison meaningful, we have scaled the two sets of data using the following expression for the absolute scattering signal:

TABLE III. Relative state-to-state cross sections for inelastic collisions of OH with HCl and CO. The errors represent one standard deviation and for OH+HCl were obtained by a weighted statistical analysis.

	Final state		OH+HCl	OH+CO
Ω	J'	ϵ	$E_{coll}=920$ cm^{-1}	$E_{coll}=985$ cm^{-1}
3/2	3/2	e	55.36±1.43	40.48±0.90
	5/2	e	6.28±0.21	5.75±0.16
	5/2	f	6.48±0.28	4.34±0.20
	7/2	e	1.76±0.15	1.88±0.07
	7/2	f	1.75±0.16	···
	9/2	e	0.49±0.10	0.44±0.05
	9/2	f	0.82±0.30	0.27±0.07
1/2	1/2	e	1.49±0.08	1.64±0.10
	1/2	f	1.47±0.20	1.23±0.12
	3/2 and 5/2	e[a]	1.78±0.12	1.70±0.12
	3/2	f	0.83±0.08	0.82±0.09
	5/2	f	1.3±0.24	0.92±0.11
	7/2	e	0.87±0.10	···

[a]The measured cross section contains contributions from both 3/2 e and 5/2 e states as the absorption lines used to probe them could not be resolved within the laser bandwidth.

$$S_f = C\int_{\text{coll. area}} \sigma_{i\to f} v_{\text{rel}}(x) n_{\text{sec}}(x) n_{\text{OH}}(x)\, dx, \tag{3}$$

where C is a constant related to the LIF detection efficiency, $\sigma_{i\to f}$ is the absolute cross section, $v_{\text{rel}}(x)$ is the relative velocity between the collision partners, and $n_{\text{sec}}(x)$ and $n_{\text{OH}}(x)$ represent the densities in the collision region of the secondary beam and OH beam, respectively. Since the masses of CO and HCl are not very different, it seems reasonable to assume that their flow patterns and hence the spatial dependences of the densities are the same. Furthermore, since the two molecular beams were obtained under the same conditions, their densities, $n_{\text{sec}}(x)$, can be replaced by the product $p_0 \cdot d^2$, where p_0 is the backing pressure and d the nozzle diameter, which is the same for both experiments. The density of the OH beam is the same in both experiments and the average relative velocities for the two systems differ by only 10%, which is within the experimental uncertainty of our measurements. We may omit the spatial integration and approximate the factors within the integral by their average values. The resulting simplified form of relation (3) may be used to correlate the relative state-to-state cross section (1) to the absolute cross sections:

$$\sigma_{i\to f}^{\text{rel}} \propto \frac{\sigma_{i\to f} v_{\text{rel}} n_{\text{sec}} n_{\text{OH}}}{n_i}. \tag{4}$$

For the reasons mentioned above, the relative velocities, the OH beam densities and the populations of the initial state from this expression, may be assumed to be approximately the same for OH+HCl and OH+CO collisions, and consequently ignored. In order to get an estimate of the magnitude of the absolute cross sections relative to each other, the mea-

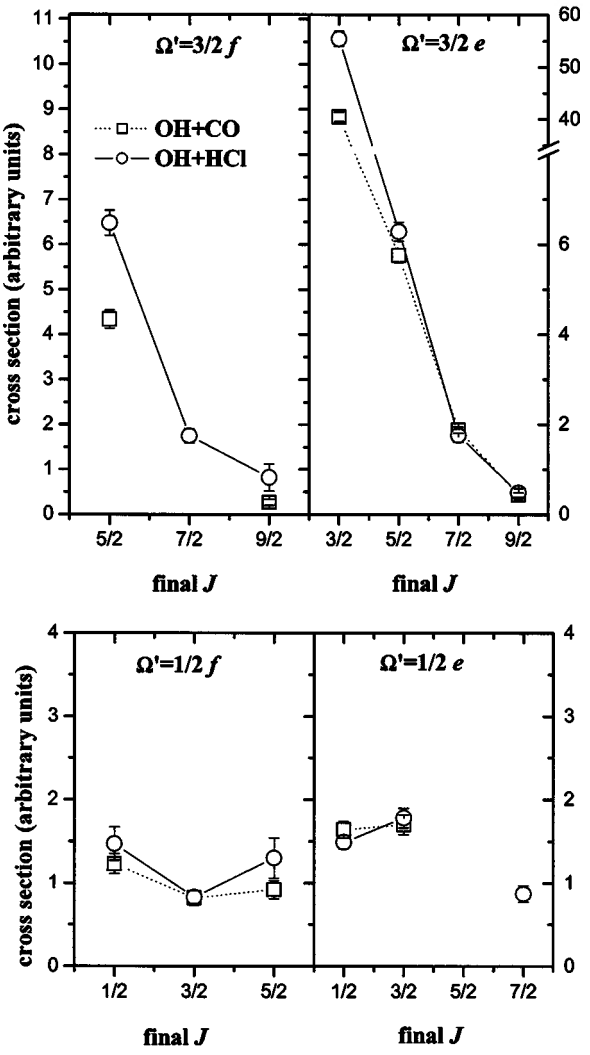

FIG. 3. Rotational dependence of the relative state-to-state cross sections for inelastic collisions of OH with HCl and CO at collision energies of 920 cm^{-1} and 985 cm^{-1}, respectively. The final spin–orbit state and the Λ-doublet symmetry are indicated at the top each panel. The cross sections for the OH+CO system are obtained by scaling as described in the text.

sured relative cross sections for CO were normalized to those for HCl simply by scaling the results with the backing pressures used in the experiments. The values obtained by this procedure are listed in Table III and plotted in Fig. 3. Within the limits of the above assumptions it can be concluded from Fig. 3 that the cross sections for collisions of OH with HCl are larger than those for collisions with CO as predicted. Unfortunately, no reliable comparison can be made between the cross sections measured at different collision energies for the OH+CO system. The two data sets cannot be scaled to each other due to the fact that they were obtained under different experimental conditions.

V. RELATION WITH THEORY

The magnitude of the inelastic cross sections and the scattering propensities are reflections of the shape of the potential energy surface (PES) governing the interaction between the collision partners. Considering the complexity of the quantum treatment of a 4-atom system, the development of a full dimensional PES is a very demanding task and the prior knowledge of the cross sections may be helpful in refining different features of the PES.

OH is an open shell molecule with a $^2\Pi$ ground state. In the absence of external fields, the doublet state is degenerate, but the approach of the collision partner lifts this degeneracy, giving rise to two electronic potential surfaces on which the collision takes place. If the collision partner is spherically symmetric (e.g., Ar), the colliding particles occupy the same plane and the two potential surfaces have either A' or A'' symmetry with respect to the reflection of the spatial electron coordinates relative to the triatomic plane. For a molecule with a π^3 electronic configuration, as is the case for the OH radical, the A' symmetry corresponds to a distribution of the single filled π orbital in the scattering plane and to a distribution of doubled filled π orbital perpendicular to this plane, whereas for the A'' symmetry the orbital distribution will be the opposite.[30] The corresponding PES's defined in the body-fixed (collision) frame may then be labeled by $V_{A'}$ and $V_{A''}$, according to their symmetry. However, when the collision partner is not spherically symmetric, as for the interaction of OH with HCl, CO or N_2, there is in general no plane of symmetry. If we restrict the discussion only to planar collision geometries it will be possible to use the above notation for the PES's and to use the scattering formalism described by Alexander[30] employing the PES's under the following forms:

$$V_{\text{sum}} = \tfrac{1}{2}(V_{A'} + V_{A''}), \tag{5}$$

$$V_{\text{dif}} = \tfrac{1}{2}(V_{A'} - V_{A''}). \tag{6}$$

They represent the matrix elements of the transformation between the adiabatic PES's, $V_{A'}$ and $V_{A''}$ and the diabatic PES's $\Pi(A')$ and $\Pi(A'')$ defined in the product molecular frame. The angular and radial dependence of the sum and the difference potential can be expressed as[25]

$$V_{\text{sum}}(R,\theta) = \sum_{l=0} V_{l0}(R) d^l_{00}(\theta), \tag{7}$$

$$V_{\text{dif}}(R,\theta) = \sum_{l=2} V_{l2}(R) d^l_{20}(\theta), \tag{8}$$

where $d^l_{00}(\theta)$ and $d^l_{20}(\theta)$ represent reduced rotation matrix elements[31] and are proportional to regular and associated Legendre polynomials, respectively, and $V_{l0}(R)$ and $V_{l2}(R)$ are expansion coefficients which describe the radial dependence of the potentials and therefore, contain information on the anisotropy of the PES. Coefficients with even l contribute to the potential surface which is head–tail symmetric with respect to the OH molecule orientation while terms with odd l contribute to the potential surface which is head–tail asymmetric. The scattering matrix depends explicitly on the $V_{l0}(R)$ and $V_{l2}(R)$ coefficients.[32] Consequently, an estimation of their relative magnitude can be obtained from the values of the relative cross sections. In the case of the OH+HCl and OH+CO systems, this estimation is only valid for the case of planar geometries. It has been found at different levels of theory[12,14,15] that for the OH–HCl interaction the most stable van der Waals complex has a planar geometry. Thus, the

information deduced from the relative cross sections should describe the potential in the vicinity of the van der Waals minimum if this region of the PES dominates the collision process.

It was shown that for a pure Hund's case (a) coupling and a triatomic collision system, the spin–orbit conserving transitions are governed by the sum potential, V_{sum}, and the spin–orbit changing transitions are governed by the difference potential, V_{dif}. OH can be treated as Hund's case (a) only for the lowest rotational levels. We therefore expect that the magnitude of the Λ-doublet cross section to be determined by the $V_{l0}(R)$ coefficients with odd l index, responsible for the change in the Λ-doublet symmetry, with the biggest contribution being made by $V_{10}(R)$. Comparing the magnitude of the relative cross sections for the $J=3/2$, Λ-doublet transitions in the OH+HCl system and in the OH+CO system, one can deduce that the $V_{10}(R)$ term is larger for collisions of OH with HCl and therefore that its PES is more anisotropic. According to the expression for the scattering matrix from Ref. 32, the excitation into the $\Omega=1/2$, $J=1/2$ states can only be induced by the $l=1$ term of the potential responsible for a change in symmetry $[V_{10}(R)]$ and the $l=2$ terms of the potential responsible for symmetry conserving transitions $[V_{20}(R)]$ and $[V_{22}(R)]$. The ratio between the cross section for scattering into the $\Omega=1/2$, $J=1/2$ state of e symmetry to the cross section for scattering into the $\Omega=1/2$, $J=1/2$ state of f symmetry is almost equal to unity. On the basis that the lower-order terms of the $V_{l0}(R)$ and the $V_{l2}(R)$ have the same sign and that the contribution of $V_{10}(R)$, $V_{20}(R)$, and $V_{22}(R)$ terms are −0.07, −0.06, and +0.44, respectively,[32] we infer that the $V_{10}(R)$ term is stronger than the other two terms. For OH+CO collisions, a propensity for the $\Omega=1/2$, $J=1/2$, e state is observed at both collision energies, indicating relatively larger $V_{20}(R)$ and $V_{22}(R)$ terms compared to $V_{10}(R)$. Once again, this is pointing towards a stronger anisotropy of the PES governing the OH+HCl interaction as compared to the PES governing the OH+CO interaction. One can notice that already for the transitions into $\Omega=1/2$, $J=1/2$, e the V_{sum} potential has a small contribution to the scattering through $V_{22}(R)$ term. The interpretation of the cross sections for higher rotational states for which the OH molecule can be treated as an intermediate case (a)–(b) or a pure case (b) of Hund has to include the contributions of both V_{sum} and V_{dif}. An estimation of the magnitude of higher terms of the PES from the comparison of the Λ-resolved cross sections for excitation into higher rotational levels is complicated by the contributions of several terms to each of them.

The anisotropic character of the potential seems to be consistent with the results of theoretical calculations, which predict the most stable structure of the van der Waals complex to be formed at the O-side, ClH–OH. This complex would have a quasilinear structure with the angle between the OH bond axis and the intermolecular axis close to the bond angle in H_2O. The depth of the van der Waals well was estimated to be in the range 870–1900 cm^{-1}.[14–16,33] For the interaction between OH and CO, it was shown experimentally and theoretically that two linear complexes, OH–CO and OH–OC, may be formed, with a dissociation energy, D_e, of 700–800 cm^{-1} and 400–500 cm^{-1}, respectively.[34–36] The e/f propensities in OH+CO collisions for excitation of OH into the $\Omega=1/2$, $J=1/2$ and $\Omega=3/2$, $J=5/2$ states indicate a preference for transitions into rotational states of e symmetry. In terms of interaction potential this corresponds to stronger even l terms and consequently to a higher head tail symmetry of the PES than in the OH+HCl interaction. Hence, a weaker anisotropy of the potential is expected for the interaction of the OH with CO than for the interaction with HCl.

VI. SUMMARY

In this paper we report relative state-to-state cross sections for inelastic scattering of OH ($X^2\Pi$) by HCl ($X^1\Sigma^+$), measured at a collision energy of 920 cm^{-1}. Prior to the collisions, the OH radicals are prepared in a single quantum state, $\Omega=3/2$, $J=3/2$, f, by means of rotational cooling in a supersonic expansion followed by an electrostatic state selection. In the absence of other experimental and theoretical data concerning this system, the results are compared in a qualitative manner with results previously obtained for the collisions of OH with CO ($E_{coll}=450$ cm^{-1}) and N_2 ($E_{coll}=410$ cm^{-1}) under similar experimental conditions. To allow for a quantitative comparison, we have also performed new measurements for the OH+CO system ($E_{coll}=985$ cm^{-1}) using the same experimental set-up. As noted previously, for collisions of OH with CO and N_2, there is a propensity for spin–orbit conserving transitions that tends to decrease with the amount of the rotational excitation. With respect to the Λ-doublet symmetry, in the collisions of OH with HCl, no propensity is found, except for the case of excitation to the highest detected rotational state ($J=9/2$) of the same spin–orbit ladder ($\Omega=3/2$), for which there is perhaps a preference for excitation into the rotational state of f symmetry. This behavior is notably different from that for collisions of OH with N_2, for which a propensity for symmetry changing excitation was found, similarly to the collisions with spherical partners studied in earlier work. For the OH+CO system, the propensity for symmetry changing excitations is much weaker and mainly apparent at low rotational excitations. This lack of preference for a Λ-doublet state is related to the shape of the PES governing the collision process and suggests that the PES is less head–tail symmetric with respect to the OH orientation for the interaction with HCl than for that with CO and N_2. More conclusive information regarding the anisotropy of the PES is obtained from measurements of the steric dependence of the state-to-state cross sections, which will be the subject of a subsequent paper.

ACKNOWLEDGMENTS

The authors wish to thank Leander Gerritsen and Peter Claus for their expert technical assistance, Dr. W. L. Meerts, Professor A. van der Avoird, and Dr. J. Kłos for stimulating discussions, and Dr. C. Vallance for reading the manuscript. Financial support from the European Commission through the RTN program (RTN Reaction Dynamics), Contract No. HPRN-CT-1999-0007, is gratefully acknowledged.

[1]R. P. Wayne, *Chemistry of Atmospheres*, 3rd ed. (Oxford University Press, Oxford, 2000).
[2]J. Warnatz, U. Maas, and R. W. Dibble, *Combustion: Physical and Chemical Fundamentals, Modeling and Simulation, Experiments; Pollutant Formation* (Springer Verlag, Berlin, 1996).
[3]M. J. Molina, L. T. Molina, and C. A. Smith, Int. J. Chem. Kinet. **16**, 1151 (1984).
[4]L. F. Keyser, J. Phys. Chem. **88**, 4750 (1984).
[5]D. Husain, J. M. C. Plane, and C. C. Xiang, J. Chem. Soc., Faraday Trans. 2 **80**, 713 (1984).
[6]A. R. Ravishankara, P. Wine, J. R. Wells, and R. L. Thompson, Int. J. Chem. Kinet. **17**, 1281 (1985).
[7]Ian. W. M. Smith and M. D. Williams, J. Chem. Soc., Faraday Trans. 2 **82**, 1043 (1986).
[8]P. Sharkey and I. W. M. Smith, J. Chem. Soc., Faraday Trans. **89**, 631 (1993).
[9]F. Battin-Leclerc, I. K. Kim, R. K. Talukdar, R. W. Portmann, A. R. Ravishankara, R. Steckler, and D. Brown, J. Phys. Chem. A **103**, 3237 (1999).
[10]N. I. Butkovskaya and D. W. Setser, J. Chem. Phys. **108**, 2434 (1998).
[11]D. Clary, G. Nyman, and E. Hernandez, J. Chem. Phys. **101**, 3704 (1994).
[12]R. Steckler, G. M. Thurman, J. D. Watts, and R. J. Bartlett, J. Chem. Phys. **106**, 3926 (1997).
[13]H.-G. Yu and G. Nyman, J. Chem. Phys. **113**, 8936 (2000).
[14]A. Rodriguez, E. Garcia, M. L. Hernandez, and A. Laganà, Chem. Phys. Lett. **360**, 304 (2002).
[15]A. Rodriguez, E. Garcia, M. L. Hernandez, and A. Laganà, Chem. Phys. Lett. **371**, 223 (2003).
[16]J. Kłos, G. Dhont, P. Wormer, and A. van der Avoird (private communication).
[17]J. Kłos, J. Aoiz, R. Cireasa, and J. J. ter Meulen, Phys. Chem. Chem. Phys. **6**, 4368 (2004).
[18]K. Schreel, J. Schleipen, A. Eppink, and J. J. ter Meulen, J. Chem. Phys. **99**, 8713 (1993).
[19]K. Schreel and J. J. ter Meulen, J. Chem. Phys. **105**, 4522 (1996).
[20]M. C. van Beek, K. Schreel, and J. J. ter Meulen, J. Chem. Phys. **109**, 1302 (1998).
[21]M. C. van Beek, J. J. ter Meulen, and M. H. Alexander, J. Chem. Phys. **113**, 628 (2000).
[22]T. D. Hain and T. J. Curtiss, J. Phys. Chem. A **102**, 9696 (1998).
[23]J. Reuss, in *Atomic and Molecular Beams Methods*, edited by G. Scoles (Oxford University Press, New York, 1998), Vol. I.
[24]R. Anderson, J. Phys. Chem. A **101**, 7664 (1997).
[25]J. Schleipen and J. J. ter Meulen, Chem. Phys. **156**, 479 (1991).
[26]D. R. Guyer, L. Hüwel, and S. R. Leone, J. Chem. Phys. **79**, 1259 (1983).
[27]J. M. Hossenlopp, D. T. Anderson, M. W. Todd, and M. I. Lester, J. Chem. Phys. **109**, 10707 (1998).
[28]M. C. van Beek and J. J. ter Meulen, Chem. Phys. Lett. **337**, 237 (2001).
[29]M. J. L. de Lange, M. Drabbels, P. T. Griffiths, J. Bulthuis, S. Stolte, and J. G. Snijders, Chem. Phys. Lett. **313**, 491 (1999).
[30]M. H. Alexander, Chem. Phys. **92**, 337 (1985).
[31]D. M. Brink and S. R. Satchler, *Angular Momentum* (Clarendon, Oxford, 1968).
[32]P. J. Dagdigian, M. H. Alexander, and K. Liu, J. Chem. Phys. **91**, 839 (1989).
[33]G. Lendvay (private communication).
[34](a) M. I. Lester, B. V. Pond, D. T. Anderson, L. B. Harding, and A. F. Wagner, J. Chem. Phys. **113**, 9889 (2000); (b) M. I. Lester, B. V. Pond, M. D. Marshall, D. T. Anderson, L. B. Harding, and A. F. Wagner, Faraday Discuss. **118**, 373 (2001).
[35]K. Kudla, A. G. Koures, L. B. Harding, and G. C. Schatz, J. Chem. Phys. **96**, 7465 (1992).
[36]H.-G. Yu, J. T. Muckerman, and T. J. Sears, Chem. Phys. Lett. **353**, 578 (2001).